Dynamic heterogeneities in a supercooled diatomic molecular system

Ricardo Palomar and Gemma Sesé*

Departament de Física i Enginyeria Nuclear, Universitat Politècnica de Catalunya, Campus Nord-Mòdul B4, c/ Jordi Girona 1-3, 08034 Barcelona, Spain

(Received 31 July 2006; published 23 January 2007)

Dynamic heterogeneities in a supercooled system of diatomic molecules with an associated dipole moment have been investigated. To this end, three-time correlation functions have been evaluated. Correlations between molecular displacements performed during consecutive time intervals are apparent at low temperatures in the β-relaxation regime, whereas they tend to disappear during the α-relaxation regime. These correlations maximize when the deviation from Gaussian dynamics takes a maximum, and they reveal the existence of different dynamic domains. Directionality of translational motions has also been studied. At low temperatures, and in the β-relaxation zone, the molecular vector displacement in a given time interval has an important component in the opposite direction of the vector displacement corresponding to the initial time interval. The amplitudes associated with this quasi-oscillatory behavior become larger as the system is cooled. Dynamic heterogeneities in reorientation have been observed in the β-relaxation regime, and it has been obtained that molecules that perform faster translational motions experience faster reorientational motions too. This effect increases as temperature decreases.

DOI: 10.1103/PhysRevE.75.011505 PACS number(s): 64.70.Pf, 61.20.Lc, 02.70.Ns

I. INTRODUCTION

Understanding the nature of molecular motions in supercooled liquids when approaching the glass transition temperature is still a challenge in statistical physics. As a result of these motions, the temperature dependence of relaxation times and transport coefficients increases and the time dependence of relaxation functions changes from exponential to stretched exponential [1]. This overall nonexponential relaxation can result from the superposition of intrinsically different nonexponential processes or from the superposition of several exponential processes with different characteristic times. The latter corresponds to a heterogeneous scenario, and it implies that there is a subset of particles that translate or rotate much farther or shorter distances than an average particle. The existence of such dynamic heterogeneities has been demonstrated experimentally in many supercooled liquids [2,3].

Several theoretical approaches have been proposed to describe the specific behavior of liquids in the supercooled state. Among them, the mode-coupling theory [4,5] describes many aspects of the dynamic behavior of a variety of supercooled systems for temperatures well above the glass transition [5–8]. This theory, though, cannot account for the dynamic heterogenenity that arises in deeply supercooled liquids. The emergence of dynamic heterogeneities is taken into account in the Adam-Gibbs approach [9], which is based on the rearrangement of molecules in regions that evolve within an increasingly cooperative regime upon cooling. Nevertheless, these regions are not clearly defined. Recently, the dynamic facilitation theory [10,11] was proposed. It considers a microscopic model in which mobile particles assist their neighbors to become mobile. However, a theory that provides insight into the molecular origin of dynamic heterogeneity is still lacking.

Computer simulations have provided relevant information concerning dynamic heterogeneities in some supercooled liquids. They have been identified in a hard-sphere system [12,13], in which a remarkable anisotropic dynamics has been observed at intermediate times. Mobile and immobile particles have been identified in a binary Lennard-Jones mixture [14], and it was obtained that they were spatially correlated too [15]. For a hard-sphere system it was shown that the non-Gaussian effects were mainly related to the heterogeneous contributions to the dynamics of the system [13]. For a binary Lennard-Jones mixture, it was found that the dynamic heterogeneity was closely related to a non-Gaussian distribution of particle displacements [14,16]. As for the molecular systems, some studies have assessed the existence of dynamic heterogeneities both translational and rotational, which appeared to be coupled [17,18]. Nevertheless, whether these results can be generalized to molecular systems characterized by different microscopic models is a matter that needs to be elucidated.

The main purpose of our paper is to analyze the relevance of dynamic heterogeneities in a supercooled diatomic molecular system. The considered molecular model requires the evaluation of long-range electrostatic interactions, as every molecular site has an associated electrostatic charge. The molecular dynamics technique [23] has been used in the study. Good agreement with most of the mode-coupling predictions has been previously encountered for this system. Signatures of dynamic heterogeneities have also been found [19].

The paper is organized as follows. In Sec. II, technical details of the simulations are presented. Heterogeneities in the dynamics of translation are analyzed in Sec. III. Some results on the directional anisotropy observed in translation are given in Sec. IV. Section V is devoted to the study of reorientational dynamics. The final section contains some concluding remarks.

*Email address: gemma.sese@upc.edu

II. SIMULATION DETAILS

The system under study is composed by diatomic molecules made up of two rigidly connected beads, which stand for the methyl group (Me) and the oxygen atom (O). The charges associated with the Me and O sites are 0.323e and −0.323e, respectively. They have been evaluated so that the molecular dipole equals that of methanol molecules, given that molecular neutrality is maintained. As for the molecular mass, it is 3% lower than that of methanol molecules. Then, our molecular model is very similar to the methanol one, but it lacks sites for hydrogen bonding. It has already been used to analyze the effects of hydrogen bonding in liquid [20] and supercooled [19] methanol. The SHAKE algorithm [21] has been used to constrain bond lengths. The intermolecular interactions have been evaluated by using the Jorgensen OPLS potential [22]. It consists of a short-range Lennard-Jones part, which has been truncated at half the box length, and an electrostatic term, which has been calculated by means of the Ewald summation [23].

The sample under study consists of 1000 molecules that have been located in a cubic box with periodic boundary conditions. The integration of the equations of motion has been performed by means of the leapfrog Verlet algorithm, with a time step of 5 fs. In an initial (N,V,T) run, the sample has been equilibrated at 298 K with a density of 0.787 g/cm^3 in order to determine the pressure, which has been calculated by following [24]. A value of 1940 atm has been obtained. Then, the sample has been quenched in a stepwise manner with $\Delta T=-5$ K. Every change in the temperature has been followed by a thermalization period of 30 ps. The quenching has been performed in the (N,P,T) ensemble at the pressure previously quoted by using the algorithm proposed by Berendsen *et al.* [25]. Along the cooling process, four temperatures have been selected (298, 208, 123, and 103 K). All of them are higher than the previously obtained mode-coupling temperature for this system ($T_c=94$ K) [19]. Additional equilibration times of 250 ps at the highest temperature and of 1750 ps at the lowest temperature have been considered. Long-time production runs of 730 ps at the highest temperature and of 5 ns at the lowest temperature have been performed in the (N,V,T) ensemble.

Mean-square displacement functions of the molecular centers of mass (MCOM) have been displayed in Fig. 1. For all temperatures, three dynamic regimes are apparent: the initial linear part, which can be associated with the ballistic regime, the long-time difusive regime or α-relaxation, and the intermediate regime or β-relaxation, which becomes a *plateau* for very low temperatures. The end of this intermediate regime takes place at times approaching t^*. For all temperatures, the first non-Gaussian parameter, defined as [26]

$$\alpha_2(t)=\frac{3\langle r^4(t)\rangle}{5\langle r^2(t)\rangle^2}-1, \tag{1}$$

exhibits a maximum at t^* that increases as temperature decreases. The t^* values obtained for our system have been gathered in Table I, together with the diffusion coefficients and the long-time relaxation times associated with the self-intermediate scattering functions and the reorientational characteristic times [19].

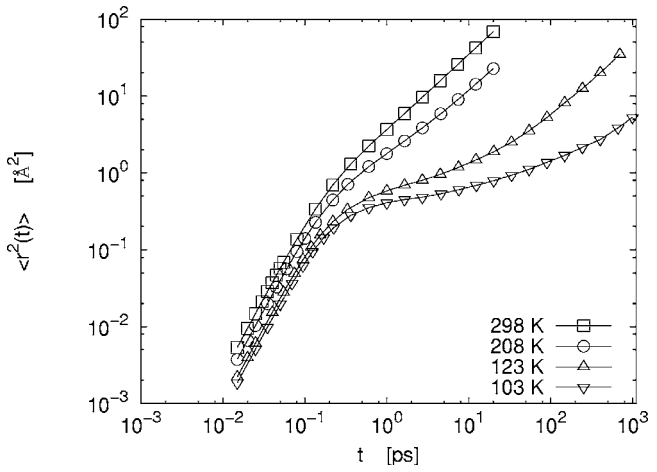

FIG. 1. $r^2(t)$ at 298, 208, 123, and 103 K.

III. HETEROGENEITY IN TRANSLATION

The nature of the nonexponential relaxation observed in our system in the supercooled state will be investigated by means of appropriately chosen three- and four-time correlation functions. They allow us to study the homogeneous and heterogeneous contributions to the overall relaxation. In a homogeneous scenario, the direction of the displacement in a given time interval depends strongly of the one undertaken in previous time steps. If translation is characterized by the existence of dynamic heterogeneities, it should be possible to select a subset of particles that translate much farther or shorter distances than an average particle. Consequently, some correlation between molecular displacements followed during consecutive time intervals should also be encountered [27].

First, we will examine the correlation between the modulus of the displacement corresponding to the MCOM in different time intervals. To this end, we have evaluated the function $\langle r_{mn}(r_{01})\rangle$ defined as

$$\langle r_{mn}(r_{01})\rangle=\int r_{mn}\frac{P_4(r_{mn},r_{01})}{P_2(r_{01})}dr_{mn}, \tag{2}$$

where $r_{01}=|\mathbf{r}_{01}|=|\mathbf{r}(t_1)-\mathbf{r}(t_0)|$ is the modulus of the displacement vector of a MCOM in a reference time interval

TABLE I. Diffusion coefficients (D), characteristic times associated with the long-time part of the self-intermediate scattering functions ($F_s(k_{\max},t)$) (τ), times corresponding to the maxima of the non-Gaussian parameter (t^*) and characteristic times associated with the molecular dipole vector autocorrelation function (τ_1), for several temperatures [19].

T (K)	D (cm^2/s)	τ (ps)	t^* (ps)	τ_1 (ps)
298	5.642×10^{-5}	0.493	1.145	0.568
208	1.819×10^{-5}	1.400	2.145	1.478
123	8.301×10^{-7}	40.142	38.41	13.186
103	6.988×10^{-8}	410.64	350.0	65.570

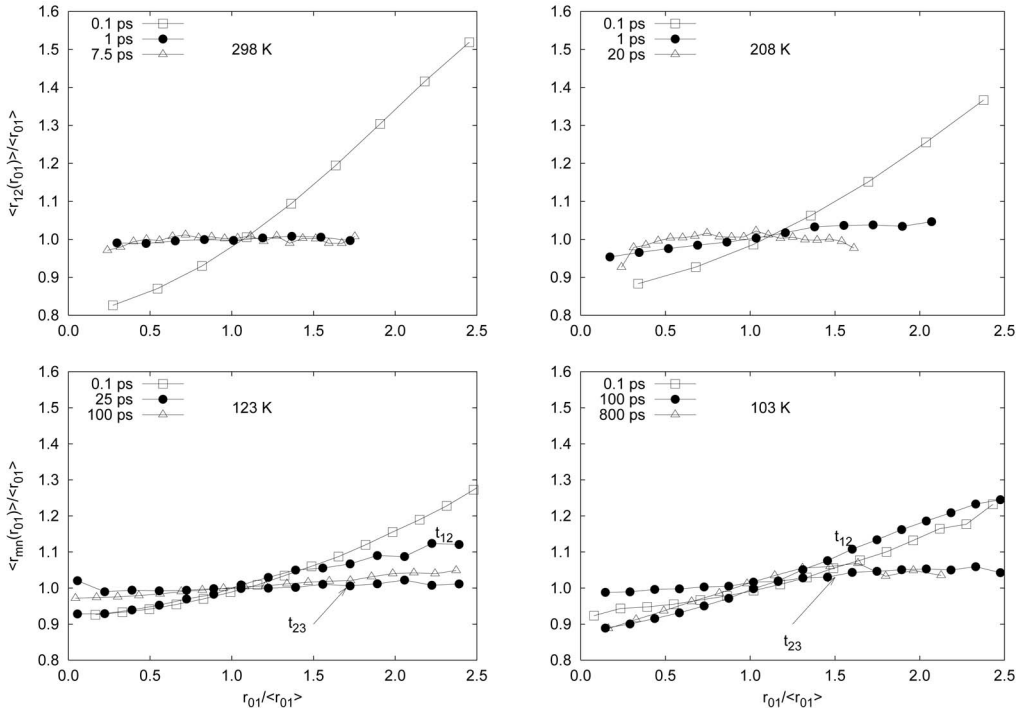

FIG. 2. $\langle r_{12}(r_{01})\rangle/\langle r_{01}\rangle$ [from Eq. (2)] against $r_{01}/\langle r_{01}\rangle$ for different time intervals t_{12} at the temperatures considered in the study. Time intervals included in the three dynamic regimes (see Sec. II) have been considered: ballistic regime (squares), β-relaxation regime (full circles), and α-relaxation regime (triangles). Please note that for 123 and 103 K, $\langle r_{23}(r_{01})\rangle/\langle r_{01}\rangle$ are also shown for the time intervals characterizing the corresponding β-relaxation regimes.

$t_{01}=t_1-t_0$, and $r_{mn}=|\mathbf{r}(t_n)-\mathbf{r}(t_m)|$ is the modulus of the displacement vector corresponding to the same MCOM in the time interval $t_{mn}=t_n-t_m$, where $n=m+1$. In our study, $\Delta t=t_{mn}=t_{01}$. Function (2) returns the r_{mn} mean value for particles that have moved a distance r_{01} during the time interval t_{01}. The joint probability $P_4(r_{mn},r_{01})$ provides the probability that the MCOM of a molecule performs a displacement r_{01} at the end of an initial time interval t_{01} and a displacement r_{mn} at the end of a later time interval t_{mn}. Even though this is a four-time correlation function, if subsequent time intervals are considered, it becomes a three-time correlation function and it can be identified as $P_3(r_{12},r_{01})$. $P_2(r_{01})$ results from the integration of $P_4(r_{mn},r_{01})$,

$$P_2(r_{01}) = \int P_4(r_{mn},r_{01})dr_{mn}. \tag{3}$$

$P_2(r_{01})$ is related to the Van Hove function through

$$P_2(r_{01}) = 4\pi r_{01}^2 G_s(r_{01},t_{01}). \tag{4}$$

It is to be noted here that $P_2(r_{01})$ obviously depends on t_{01}, and that $P_4(r_{mn},r_{01})$ and $P_3(r_{12},r_{01})$ depend on t_{mn} and t_{01} and on t_{12} and t_{01}, respectively. Such dependences have been omitted for the sake of simplicity.

Some $\langle r_{mn}(r_{01})\rangle$ functions are displayed in Fig. 2 for the temperatures under study. Their behavior strongly depends on the considered time interval. Then, the three distinct zones outlined in Sec. II that characterize the dynamics of the system will be investigated.

In the ballistic regime ($\Delta t=0.1$ ps), $\langle r_{mn}(r_{01})\rangle$ functions display the same qualitative behavior for all temperatures. During this regime, the influence of the surrounding molecules on the dynamics of a given molecule is still very small. At room temperature, molecules that have performed displacements over the average at the end of t_{01} have the same behavior at the end of the following three time intervals. This result is a consequence of the inertial effects associated with the individual dynamics of molecules. Upon cooling the system, the individual dynamics becomes slower on average, and the number of time intervals required for a given molecule to overcome the inertial effects increases slightly. Similar trends are observed for molecules that have performed displacements under the average at the end of t_{01}.

The behavior of $\langle r_{mn}(r_{01})\rangle$ has also been analyzed for time intervals approaching t^*, that is, in the so-called β-relaxation regime. It is apparent in Fig. 2 that at room temperature (with $\Delta t=1$ ps), $\langle r_{12}(r_{01})\rangle/\langle r_{01}\rangle \approx 1$, independently of the r_{01} value. Nevertheless, upon cooling the system, $\langle r_{mn}(r_{01})\rangle$ becomes clearly dependent on r_{01}. At 208 K, $\langle r_{12}(r_{01})\rangle$ depends on r_{01}: molecules that have performed displacements under the average during t_{01} have also done so during t_{12}. They can be termed as *slow* molecules. Accordingly, molecules that have performed displacements over the average during t_{01} have also done so during t_{12} (*fast* molecules). This effect becomes more important at lower temperatures. For 123 and 103 K, with $\Delta t=25$ and 100 ps, respectively, *fast* molecules at the end of t_{01}, are also *fast* molecules not only up to t_{12}, but also at the end of t_{23}, as shown in Fig. 2, where $\langle r_{23}(r_{01})\rangle/\langle r_{01}\rangle$ are also shown. The same applies to the *slow* molecules.

Then, as the system is cooled toward its glass transition, different dynamic domains appear in the system. These dynamic heterogeneities exist at intermediate times and they characterize the dynamics during the β-relaxation regime at low temperatures.

As for the results obtained in the α-relaxation zone, some hints of the existence of different dynamic domains appear only at the lowest temperature analyzed. Nevertheless, the slope associated with $\langle r_{12}(r_{01})\rangle$ for $\Delta t=800$ ps is smaller than the one obtained when time intervals close to t^* are considered. This result can be understood by taking into account that diffusive processes that are characteristic of this regime tend to homogenize the system, even at low temperatures.

Let us now focus on the analysis of the dynamics in two consecutive time intervals. Then, a characterization of the dynamic domains is required. A molecule will be considered as *slow* if its associated displacement at the end of a time interval Δt is smaller than a characteristic distance d_s. Alternatively, a molecule will be considered as *fast* if its displacement at the end of a time interval Δt is larger than a characteristic distance d_f. Both distances d_s and d_f have been evaluated for every time interval so that the 7% most mobile molecules and the 7% least mobile molecules have been selected for further analysis. Molecular fractions ranging between 5% and 8% were used in the study of spatially correlated dynamics of a model polymer melt [28]. It was shown that the qualitative features of the results did not depend on the exact figure considered. Thus, the probability of finding a *fast* molecule at the end of the time interval t_{01} is

$$P(T_{f,01}) = \int_0^\infty dr_{12} \int_{d_f}^\infty P_3(r_{12},r_{01}) dr_{01} = 0.07, \qquad (5)$$

which allows us to evaluate d_f. A similar equation can be written for the *slow* molecules, and d_s can also be evaluated. The probability that a molecule can be termed as *fast* during two consecutive time intervals can be obtained by the following:

$$P(T_{f,12} \cap T_{f,01}) = \int_{d_f}^\infty dr_{12} \int_{d_f}^\infty P_3(r_{12},r_{01}) dr_{01}. \qquad (6)$$

A similar approach permits us to analyze the probability that a *slow* molecule during t_{01} can still be considered as *slow* at the end of t_{12}. The dynamic memory of *fast* molecules has been analyzed by means of the parameter

$$\Gamma_f = \frac{P(T_{f,12} \cap T_{f,01})}{P(T_{f,01})}. \qquad (7)$$

$\Gamma_s(\Delta t)$ is the analogous quantity for the *slow* molecules. Functions $\Gamma_f(\Delta t)$ and $\Gamma_s(\Delta t)$ have been displayed in Fig. 3. $\Gamma_f(0)=\Gamma_s(0)=1$, and inertial dynamics is observed for very short time intervals. For very large time intervals, no correlation exists between the dynamic trends observed in consecutive time intervals, $P(T_{f,12} \cap T_{f,01})=P(T_{f,01})P(T_{f,12})$ and $\Gamma_{f,s}(\Delta t \to \infty)=0.07$. For intermediate times, and at room temperature, both functions decrease as Δt increases. The behavior changes qualitatively at 123 K and 103 K. At these temperatures and for time intervals included in the β-relaxation regime, the Γ_f functions increase, reach maximum values, and then decrease toward their limiting value for time intervals already in the α-relaxation regime. At 123 K, up to 15% of the molecules initially termed as *fast* are still so, and this proportion can be as large as 17% at 103 K. Similar orders of magnitude were obtained for silica [29], which suggests that this property depends only mildly on the system under consideration. The same qualitative trends are observed for $\Gamma_s(\Delta t)$, the dynamic memory being slightly shorter for the *slow* molecules.

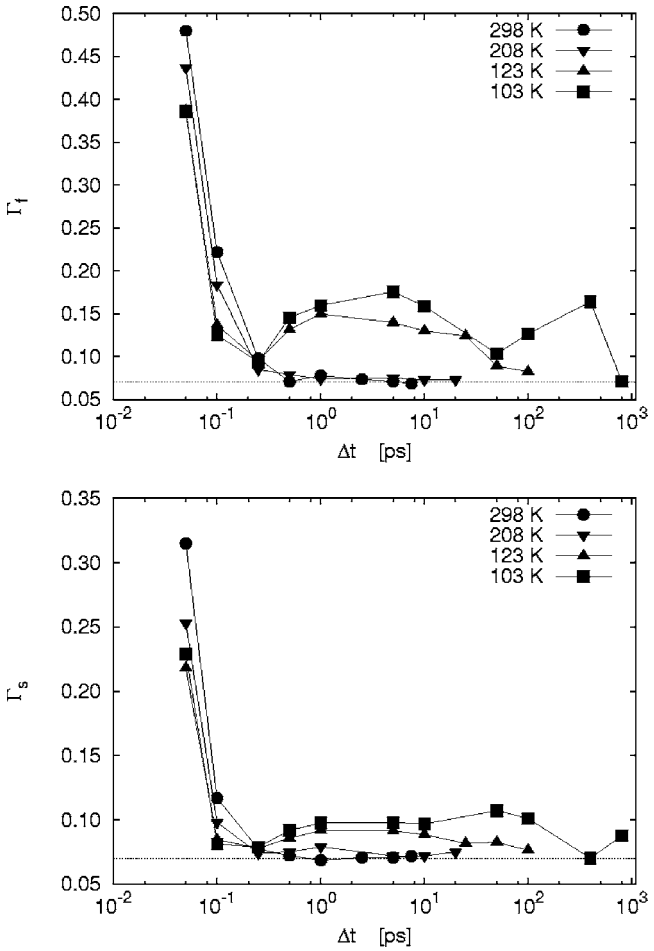

FIG. 3. $\Gamma_f(\Delta t)$ and $\Gamma_s(\Delta t)$ [see Eq. (7) in Sec. III] for different temperatures.

In order to analyze the mutual dependence between displacements in consecutive time intervals r_{01} and r_{12}, we have evaluated the distribution covariance

$$c = \int (r_{01} - \langle r_{01}\rangle)(r_{12} - \langle r_{12}\rangle) P_3(r_{12},r_{01}) dr_{01} dr_{12}. \qquad (8)$$

Taking into account that

$$\langle r_{01} r_{12}\rangle = \int r_{01} r_{12} P_3(r_{12},r_{01}) dr_{01} dr_{12}, \qquad (9)$$

Eq. (8) can be rewritten as

$$c = \langle r_{01} r_{12}\rangle - \langle r_{01}\rangle\langle r_{12}\rangle. \qquad (10)$$

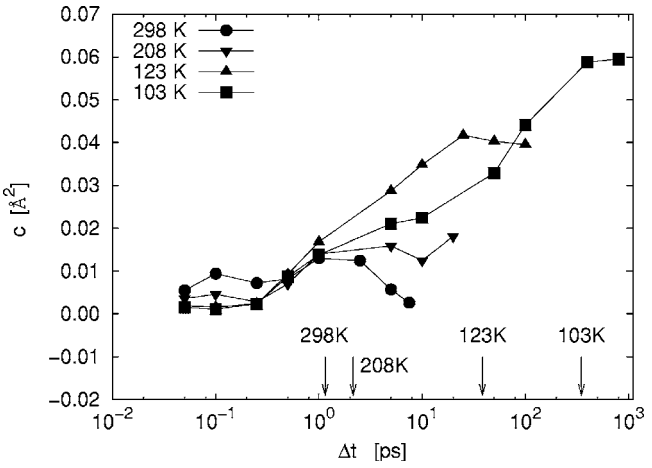

FIG. 4. Covariance defined in Eq. (8) against Δt for different temperatures. t^* values (see Table I) are indicated in the time axis with arrows.

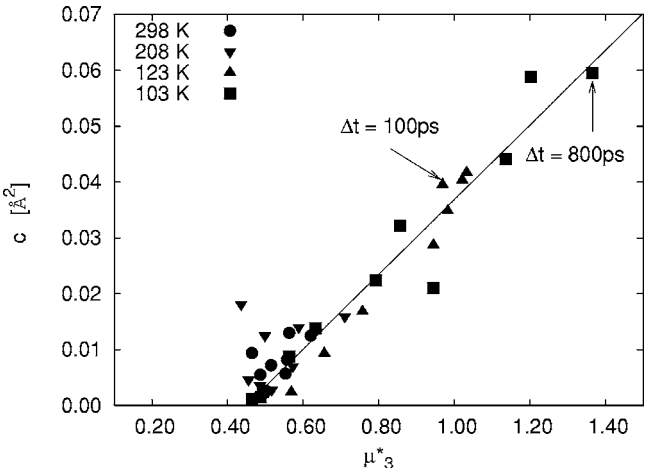

FIG. 5. Covariance [Eq. (8)] against μ_3^* [Eq. (13)].

The covariance c is displayed in Fig. 4 as a function of Δt. It always takes positive values, which indicates that r_{01} displacements over (under) the average are associated with r_{12} displacements over (under) the average too. At room temperature, c increases as larger Δt are considered. For $\Delta t \to \infty$, r_{01} and r_{12} become independent and $c=0$. Between these limiting values, c reaches a maximum when $\Delta t \approx t^*$. Similar trends are followed qualitatively when the temperature decreases. Upon cooling the system, the c maxima become more important.

The centered moments associated with the statistical distribution of molecular displacements (μ_n) have been evaluated to get an insight into the relationship between dynamic heterogeneities and deviations from Gaussianity. They have been obtained by the following:

$$\mu_n = \int_0^\infty (r - \langle r \rangle)^n P_2(r) dr. \tag{11}$$

If the Gaussian approximation is considered for the Van Hove function, Eq. (4) becomes

$$P_{2G}(r_{01}) = 4\pi r_{01}^2 \left(\frac{b}{\pi}\right)^{3/2} \exp(-br^2), \tag{12}$$

where the parameter b depends on time. The centered moments associated with Eq. (12) can be evaluated by replacing $P_2(r)$ by $P_{2G}(r_{01})$ in Eq. (11). The corresponding second and third centered moments are $\mu_{2G}=0.2268/b$ and $\mu_{3G}=0.0524/b^{3/2}$, respectively. Consequently, it is possible to calculate the nondimensional coefficient

$$\mu_3^* = \frac{\mu_3}{\mu_2^{3/2}}, \tag{13}$$

which for a Van Hove Gaussian distribution is equal to $\mu_{3G}^*=0.486$. Then, deviations from this value are associated with deviations from Gaussian behavior. It has been obtained that for very short time intervals $\mu_3^* \approx \mu_{3G}^*$, whereas much larger μ_3^* values are reached when long time intervals are considered, especially at low temperatures.

Covariance and μ_3^* values are displayed in Fig. 5. It is apparent that both larger deviations from μ_{3G}^* and larger values for c take place at the lower temperatures. A linear relationship between c and μ_3^* is apparent in the figure, which means that the more important the deviations from Gaussianity are, the more relevant the dynamic heterogeneities are. That is, both quantities are intrinsically associated. Connection between both magnitudes was also observed in a hard-spheres system [13] and in a binary Lennard-Jones mixture [16].

IV. ANISOTROPY IN TRANSLATION

It was previously obtained that translational motions in our system are not isotropic until the end of the α-relaxation regime. For earlier dynamic regimes, the component of the displacement in the direction of the dipole moment is larger than the perpendicular one [19]. We will analyze whether there is any correlation in the direction of motion between displacements performed during consecutive time intervals by means of the evaluation of the three-time correlation function $\langle r_{\parallel,12}(r_{01}) \rangle$, defined as

$$\langle r_{\parallel,12}(r_{01}) \rangle = \int \mathbf{r}_{12} \cdot \frac{\mathbf{r}_{01}}{r_{01}} \frac{P_{\parallel,4}(r_{\parallel,12}, r_{01})}{P_2(r_{01})} dr_{\parallel,12}. \tag{14}$$

$r_{\parallel,12}$ is the projection of $\mathbf{r}_{12}$ onto the direction defined by $\mathbf{r}_{01}$. $P_{\parallel,4}(r_{\parallel,12}, r_{01})$ gives the probability of having a displacement projection along the $\mathbf{r}_{01}$ direction equal to $r_{\parallel,12}$ at the end of the time interval t_{12}. Then, function (14) returns the mean value of the projection of $\mathbf{r}_{12}$ onto the direction given by $\mathbf{r}_{01}$. $\langle r_{\parallel,12}(r_{01}) \rangle$ functions for different time intervals have been displayed in Fig. 6.

For all temperatures, large values of $r_{\parallel,12}$ are associated with large values of r_{01} when very short time intervals are considered ($\Delta t=0.1$ ps), which is the result of the inertial effects characterizing the initial stages of the movement. On the other hand, after time intervals close to the characteristic times associated with the α-relaxation process (see Table I)

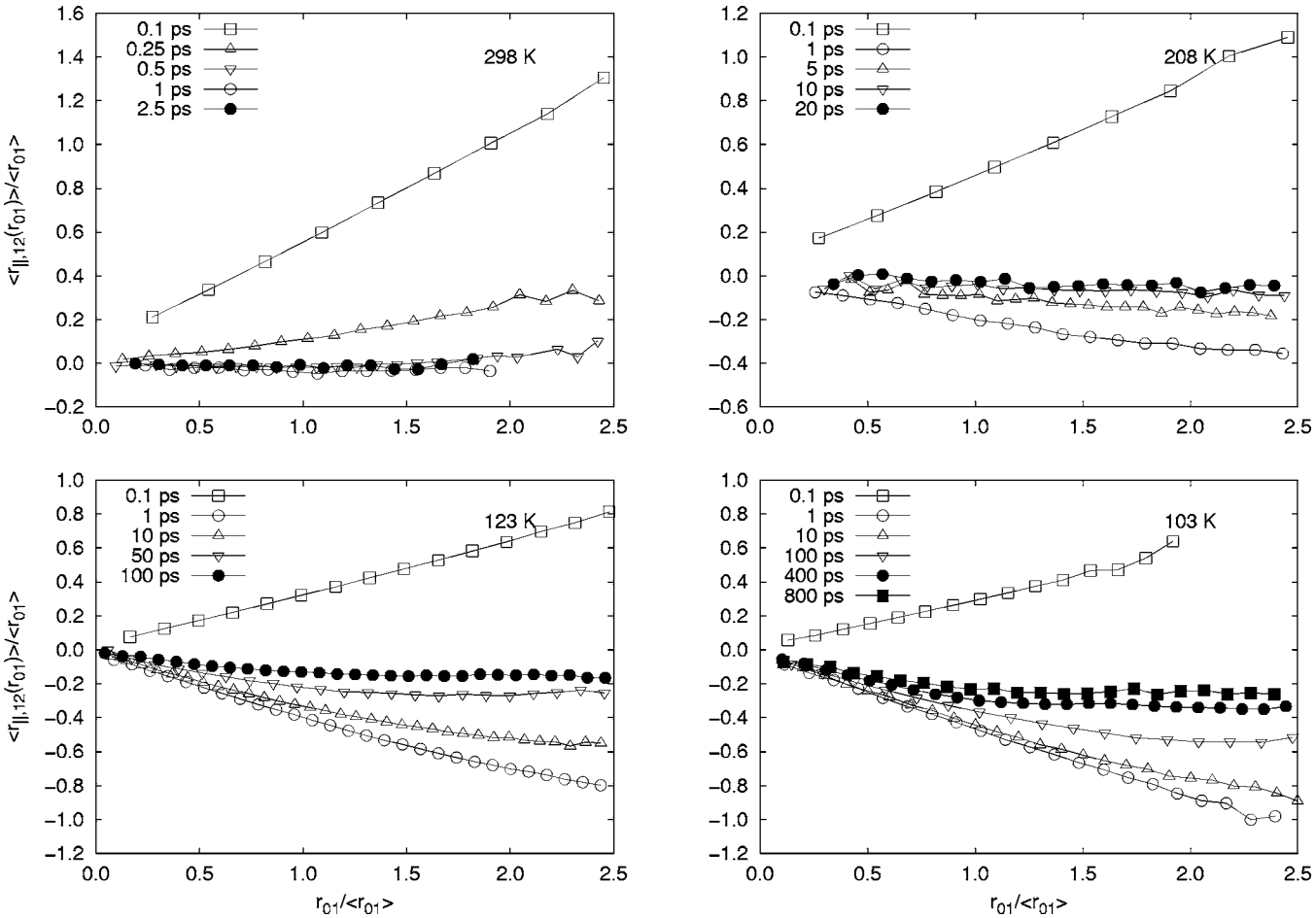

FIG. 6. $\langle r_{\parallel,12}(r_{01})\rangle$ [Eq. (14)] against $r_{01}/\langle r_{01}\rangle$ for different time intervals t_{12}.

have elapsed, the MCOM dynamics becomes independent of $\mathbf{r}_{01}$.

At room temperature and for very short time scales, $\langle r_{\parallel,12}(r_{01})\rangle$ functions take positive values. They go to zero at about $\Delta t \approx 1$ ps, which shows that the correlation with the direction of the displacement in t_{01} has completely disappeared. Upon cooling the system, and for time intervals in the β-relaxation regime, $\langle r_{\parallel,12}(r_{01})\rangle$ show negative slopes. In this regime, on average, the vector displacement of a molecule has an important component in the opposite direction of the vector displacement observed during the t_{01} time interval. The corresponding amplitudes, relative to the initial displacement r_{01}, become larger as the system is cooled. This is consistent with the picture of molecules moving in the cage made up by their nearest neighbors, and with this dragging back effect being more important as the system approaches the glass transition. Maximum amplitudes are encountered at the initial stages of the β-relaxation regime (for $\Delta t \approx 1$ ps). For larger Δt, the dynamics of a given molecule cannot be described only by the purely dragging back effect, which leads to lower values for the projection of the MCOM displacement along the $\mathbf{r}_{01}$ direction.

It is interesting to note that the dragging back effect observed in the β-relaxation regime can be modeled as

$$\langle r_{\parallel,12}(r_{01})\rangle = \begin{cases} q r_{01}, & r_{01} < D_c \\ q D_c, & r_{01} \geq D_c. \end{cases} \tag{15}$$

This behavior was also observed in a hard-spheres system [12,13]. An approximate value for D_c can be obtained from the $\langle r_{\parallel,12}(r_{01})\rangle$ functions at 123 and 103 K. According to Fig. 6, for 123 K and $\Delta t = 10$ ps, $D_c \approx 1.6\langle r_{01}\rangle$. For 103 K and $\Delta t = 100$ ps, $D_c \approx 1.5\langle r_{01}\rangle$. Taking into account the $\langle r_{01}\rangle$ values, which have been gathered in Table II, $D_c \approx 1.6$ Å holds for both temperatures. As for displacements larger than D_c the backdragging effect decreases, this distance can be considered as an estimate for the cage dimensions. The D_c value is consistent with the results obtained for the COM radial distribution functions as it is smaller than the first maximum width [19]. The quantity $D_c/2$, which should be associated with the radius of the cage, is close to the distance where the dynamics starts to be fully diffusive, as is shown in Fig. 1.

As for the q values, for 123 K and $\Delta t = 10$ ps, it has been obtained that $q = -0.33$. For 103 K and $\Delta t = 100$ ps, $q = -0.35$. The observed value for a system driven by a harmonic potential is -0.5 [30]. This result indicates that the dynamics in our system during the β-relaxation regime has a remarkable oscillatory behavior, especially at very low temperatures. Significant quasiharmonic motion in this regime

TABLE II. Mean displacement given in Å ($\langle r_{01}\rangle$) of the molecular centers of mass corresponding to different time intervals t_{01} for several temperatures.

t_{01} (ps)	$T=298$ K	$T=208$ K	$T=123$ K	$T=103$ K
0.1	0.367	0.295	0.242	0.239
0.25	0.782	0.609	0.452	0.403
0.5	1.179	0.874	0.577	0.496
1.0	1.682	1.160	0.670	0.548
2.5	2.636			
5.0	3.696	2.201	0.872	0.630
7.5	4.518			
10		3.027	1.015	0.666
20		4.154		
25			1.259	
50			1.576	0.930
100			2.086	1.030
400				1.473
800				1.657

was also found in supercooled water studies [7]. It would be interesting to analyze this behavior in terms of the topography of the potential energy landscape (PEL) [31]. It seems likely that, in the β-relaxation time scale, the system spends a lot of time hopping back and forth between two local minima of the PEL. Further investigation would be required to confirm this.

V. HETEROGENEITY IN THE REORIENTATIONAL DYNAMICS

The reorientational dynamics has been analyzed by means of the study of the time dependence of m_{01}, defined as

$$m_{01} = \mathbf{u}(t_1) \cdot \mathbf{u}(t_0), \tag{16}$$

where $\mathbf{u}(t)$ is the unit vector in the direction of the molecular bond. Then, m_{01} gives information about the molecular reorientation at the end of the time interval t_{01}. It is obtained that the limiting value for $\langle m_{01}\rangle$ is zero for long time intervals, which indicates that all orientations have the same occurrence probability, independently of the molecular orientation at t_0. Reorientational motions are very fast at room temperature and the long-time regime is reached after a few picoseconds have elapsed. Reorientational motions are hindered as the system is cooled, and time intervals of several hundred picoseconds are needed to reach the long-time regime at the lowest analyzed temperature.

The issue of the existence of reorientational heterogeneities and their correlation with translational heterogeneities has also been analyzed by means of the joint probability

$$\langle m_{01}(r_{01})\rangle = \int m_{01} \frac{P_2(m_{01}, r_{01})}{P_2(r_{01})} dm_{01}, \tag{17}$$

where $P_2(m_{01}, r_{01})$ is the probability of having a molecular reorientation characterized by m_{01} during the time interval t_{01} whereas its molecular displacement is r_{01} during the same time interval. $\langle m_{01}(r_{01})\rangle$ functions for several time intervals are displayed in Fig. 7. For all temperatures, they are independent of r_{01} in the ballistic regime, and they go to zero when long time intervals are considered. For intermediate time scales, molecules with larger r_{01} values have smaller m_{01} values, which should be associated with larger reorientational motions. Then, molecules that translate faster will also reorient faster. This effect is more important at very low temperatures, especially for intermediate time scales. This is apparent in Fig. 7, in the results obtained at $T=123$ K with $\Delta t=10$ ps and in the ones at $T=103$ K with $\Delta t=10$ ps and $\Delta t=100$ ps, all of them in the β-relaxation regime.

In order to identify *fast* molecules from a reorientational point of view, a similar approach to the one followed in Sec. III has been used. The probability that a molecule is reorientationally fast (*r-fast*) is

$$P(R_{f,01}) = \int_0^\infty dr_{01} \int_{m_f}^{m_l} P_2(m_{01}, r_{01}) dm_{01}, \tag{18}$$

where the m_f constant has been chosen so that only 7% of the total amount of molecules are considered as *r-fast*. That is, $P(R_{f,01})=0.07$. As the largest change for the angle characterizing molecular reorientation is π rad, it has been considered that $m_l=\cos\pi=-1$.

The probability that a molecule is *fast* both in translation and in reorientation can be evaluated from

$$P(R_{f,01} \cap T_{f,01}) = \int_{d_f}^\infty dr_{01} \int_{m_f}^{m_l} P_2(m_{01}, r_{01}) dm_{01}. \tag{19}$$

The coupling between reorientation and translation has been studied by means of the parameter

$$\eta_f = \frac{P(R_{f,01} \cap T_{f,01})}{P(T_{f,01})}. \tag{20}$$

For a complete decoupling, $P(R_{f,01} \cap T_{f,01}) = P(R_{f,01})P(T_{f,01})$ and $\eta_f=0.07$. The η_f parameter has been displayed in Fig. 8 for different time intervals. A complete decoupling between translation and reorientation is observed for short and very long time intervals. For all temperatures, the parameter takes a maximum for time intervals located in the early β-relaxation regime, and then decreases. In this regime, the coupling increases as temperature decreases, and so does the value corresponding to the maximum.

VI. CONCLUDING REMARKS

Dynamic heterogeneities have been investigated in a supercooled system composed by diatomic molecules with an associated dipole moment. They characterize the system dynamics during the β-relaxation regime at low temperatures. Then, it becomes possible to distinguish between *slow* and *fast* molecules in this regime. Larger deviations from a Gaussian behavior are associated with the existence of more relevant dynamic heterogeneities. Diffusive processes, which are characteristic of the α-relaxation regime, tend to homogenize the system, even at low temperatures, and the mol-

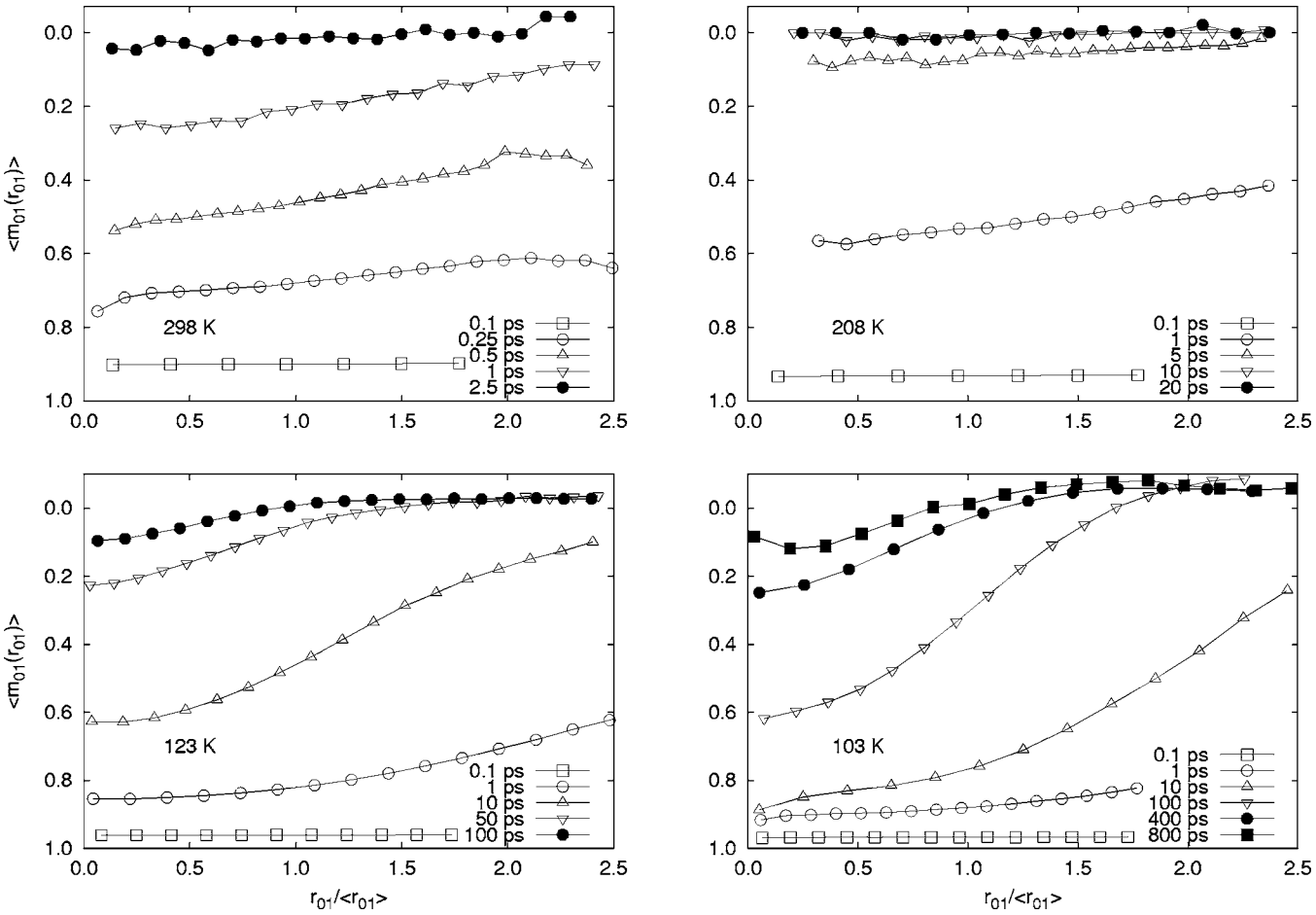

FIG. 7. $\langle m_{01}(r_{01})\rangle$ [Eq. (17)] against $r_{01}/\langle r_{01}\rangle$ for several time intervals.

ecules lack dynamic memory on the corresponding time scales.

In the study of the translation dynamics for time scales corresponding to the β-relaxation, it is interesting to note that the dynamic memory of *slow* molecules is shorter than that of *fast* molecules. In this regime, on average, the vector displacement of a molecule has a relevant component in the opposite direction of the vector displacement followed during the reference time interval, which denotes a remarkable oscillatory behavior. The corresponding amplitudes become larger as the system is cooled. This is consistent with the picture of molecules moving in the cage made up by their nearest neighbors, and with this dragging back effect being more important as the system approaches the glass transition. From the modeling of the dragging back effect, an estimate for the radius of the cage has been given, which is very similar to the distance at which the dynamics starts to be fully diffusive.

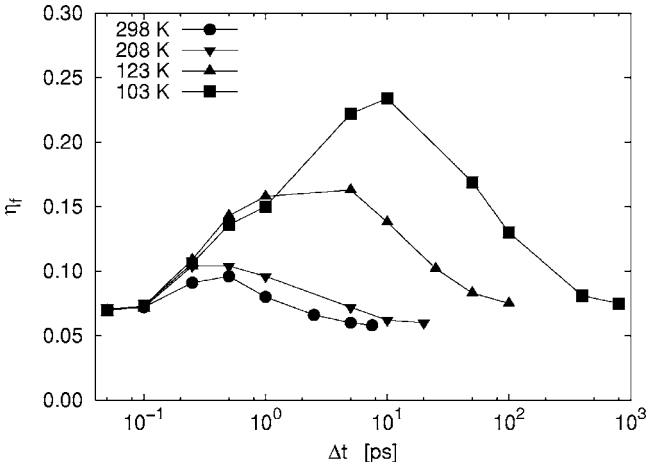

FIG. 8. η_f [Eq. (20)] against the considered time intervals, for different temperatures.

The issue of the existence of reorientational heterogeneities and their correlation with translational heterogeneities has also been analyzed. It has been found that molecules that translate faster, reorientate faster too for intermediate time scales, that is, in the β-relaxation regime. The coupling between translation and reorientation increases as the temperature decreases. A complete decoupling is observed both in the ballistic and in the diffusive dynamic regimes.

ACKNOWLEDGMENTS

Financial support from DGICYT (Project BFM2003-08211-C03-01/FISI) and Generalitat de Catalunya (Project 2005SGR 00779) is gratefully acknowledged.

[1] *Disorder Effects on Relaxational Processes*, edited by R. Richert and A. Blumen (Springer, Berlin, 1994).
[2] H. Sillescu, J. Non-Cryst. Solids **81**, 243 (1999).
[3] M. D. Ediger, Annu. Rev. Phys. Chem. **51**, 99 (2000).
[4] W. Götze, in *Liquids, Freezing and the Glass Transition*, edited by J. P. Hansen, D. Levesque, and J. Zinn-Justin, Session LI, Les Houches, 1989 (North Holland, Amsterdam, 1991).
[5] W. Kob, in *Supercooled Liquids: Advances and Novel Applications*, edied by J. T. Fourkas, D. Kivelson, U. Mohanty, and K. A. Nelson. ACS Symposium Series (1997), Vol. 676, p. 28.
[6] L. J. Lewis and G. Wahnström, Phys. Rev. E **50**, 3865 (1994).
[7] F. Sciortino, P. Gallo, P. Tartaglia, and S. H. Chen, Phys. Rev. E **54**, 6331 (1996).
[8] G. Sesé and R. Palomar, J. Chem. Phys. **114**, 9974 (2001).
[9] G. Adam and J. H. Gibbs, J. Chem. Phys. **43**, 139 (1965).
[10] J. P. Garrahan and D. Chandler, Phys. Rev. Lett. **89**, 035704 (2002).
[11] J. P. Garrahan and D. Chandler, Proc. Natl. Acad. Sci. U.S.A. **100**, 9710 (2003).
[12] B. Doliwa and A. Heuer, Phys. Rev. Lett. **80**, 4915 (1998).
[13] B. Doliwa and A. Heuer, J. Phys.: Condens. Matter **11**, A277 (1999).
[14] W. Kob, C. Donati, S. J. Plimpton, P. H. Poole, and S. C. Glotzer, Phys. Rev. Lett. **79**, 2827 (1997).
[15] C. Donati, S. C. Glotzer, P. H. Poole, W. Kob, and S. J. Plimpton, Phys. Rev. E **60**, 3107 (1999).
[16] M. Scott Shell, P. G. Debenedetti, and F. H. Stillinger, J. Phys.: Condens. Matter **17**, S4035 (2005).
[17] J. Qian, R. Hentschke, and A. Heuer, J. Chem. Phys. **110**, 4514 (1999).
[18] M. G. Mazza, N. Giovambattista, F. W. Starr, and H. E. Stanley, Phys. Rev. Lett. **96**, 057803 (2006).
[19] R. Palomar and G. Sesé, J. Phys. Chem. B **109**, 499 (2005).
[20] E. Guàrdia, G. Sesé, and J. A. Padró, J. Mol. Liq. **62**, 1 (1994).
[21] J. P. Ryckaert, G. Cicotti, and H. J. C. Berendsen, J. Comput. Phys. **23**, 327 (1999).
[22] W. L. Jorgensen, J. Phys. Chem. **90**, 1276 (1986).
[23] M. P. Allen and D. J. Tildesley, *Computer Simulation of Liquids* (Clarendon Press, Oxford, 1987).
[24] G. Hummer, N. Gronbech-Jensen, and M. Neumann, J. Chem. Phys. **109**, 2791 (1998).
[25] H. J. C. Berendsen, J. P. M. Postma, W. F. van Gunsteren, A. DiNola, and J. R. Haak, J. Chem. Phys. **81**, 3684 (1984).
[26] J. P. Boon and S. Yip, *Molecular Hydrodynamics* (Dover Publications, New York, 1991).
[27] A. Heuer and K. Okun, J. Chem. Phys. **106**, 6176 (1997).
[28] Y. Gebremichael, T. B. Schroder, F. W. Starr, and S. C. Glotzer, Phys. Rev. E **64**, 051503 (2001).
[29] M. Vogel and S. C. Glotzer, Phys. Rev. Lett. **92**, 255901 (2004).
[30] A. Heuer, M. Kunow, M. Vogel, and R. D. Banhatti, Phys. Rev. B **66**, 224201 (2002).
[31] M. Goldstein, J. Chem. Phys. **51**, 3728 (1969).